Exp. Theo. NANOTECHNOLOGY 10 (2026) 441-452 https://doi.org/10.56053/10.2.441

Antibacterial and antioxidant activity of gamma star-like MnO_2 nanostructure with and without coating with iron oxide nanoparticles

Gulboy Abdolmajeed Nasir[1], *Zahraa Hasan Raheem*[1], *Huda Musleh Mahmood*[2,*], *Suhayla Khalid Mohammed*[1]

[1]College of Agricultural Engineering Sciences, University of Baghdad, Baghdad, Iraq
[2]Department of Biotechnology, College of Sciences, University of Anbar, Ramadi, Iraq
[*)] Email: huda.mahmood@uoanbar.edu.iq

Received 2/1/2026, *Received in revised form* 13/3/2026, *Accepted* 29/3/2026, *Published* 15/4/2026

Bacterial resistance caused by antibiotic misuse has garnered substantial attention, prompting numerous researchers to develop materials that can combat these resistant pathogens. The hydrothermal method is employed to produce γ-MnO_2 nanostars and to coat them with Fe_2O_3 nanoparticles. The materials are characterized using XRD, FE-SEM, EDX, and UV-vis spectrophotometry, as well as antioxidant and antibacterial activities. The nano γ-MnO_2 star shapes are coated with tiny spherical Fe_2O_3 nanoparticles with diameters of 35-47 nm. The peaks located at the crystal planes (120), (031), (131), (230), (300), (160), (421), and (003) are represented by the values of 2θ = 22.36º, 34.36º, 37.22º, 38.78º, 42.56º, 56.14º, 65.48º and 68.82º, respectively, and no additional peaks for any more materials showing pure γ-MnO_2. The SEM descriptions of the star shapes of γ-MnO_2 nanostructure in three different magnifications. The diameters of the six-branched star-shaped γ-MnO_2 are about 140 nm close to the star's center, 55–70 nm close to its tips, and 1.5–4 μm in length. The EDX analysis of the γ-MnO_2 nanostars are coated with Fe_2O_3 nanoparticles. It clearly shows the elemental composition that includes Mn, O, and Fe. The radical scavenging performance of the γ-MnO_2 nanostars coated with Fe_2O_3 nanoparticles is showed substantial enhancement compared to bare γ-MnO_2 nanostars. The prepared materials exhibit comparable antibacterial properties, with noticeable activity against Gram-negative strains (*Salmonella and Escherichia coli*), but no effectiveness against Gram-positive strains (*Bacillus subtilis and Staphylococcus aureus*).

Keywords: γ-MnO_2 nanostars; Fe_2O_3; Scavenging activity; Antimicrobial efficacy.

1. INTRODUCTION

Nanoparticles possess unique size-dependent characteristics that add value in various fields, including cosmetics, agriculture, and the medical field [1-3]. They can be synthesized in three ways: physically, chemically, or biologically, with the latter being safer and more environmentally friendly [4]. Nanomaterials are substances with external dimensions of one or more nanometers [5,6]. Today, a variety of types are used as substitutes for traditional antibiotics, especially nanocomposites, because of their exceptional chemical and physical features and substantial potential as antibacterial agents [7], including silver nanoparticles [8], gold nanoparticles [8,9], zinc oxide [10,11], titanium dioxide nanoparticles [12,13], and bismuth nanoparticles [14]. Due to their unique qualities and increased surface area- to- volume ratio, manganese dioxide, particularly nanostructured MnO_2, has gained much attention and can be effectively used in many applications, such as an electrode material in alkaline batteries [15], dye production [16], gas sensors [17], solar cells [18,19], wastewater treatment [20,21], biological applications [22,23], and supercapacitors [24]. The functionality of MnO_2 varies because of different crystallographic forms, including δ, γ, α, β, λ, and ε, as well as its natural abundance, notable electrochemical properties, low cost, and environmental friendliness [25]. γ-MnO_2 is often used as a cathode material in lithium and alkaline batteries due to its outstanding structure and pronounced electrochemical activity, along with other previously mentioned properties [26]. As proposed by De Wolff, the complex structure of γ-MnO_2 can be understood as a random intergrowth of varying proportions of the pyrolusite phase (1 x 1) within the ramsdellite phase [27]. Applications of MnO_2 nanostructures include pure MnO_2 nanostructures or those doped or combined with other materials or polymers [26,28].

Although traditional antibiotics are commonly used to treat bacterial infections, excessive use can lead to bacterial resistance and increased illness [28]. Some studies on biosynthesized MnO_2 nanostructures have shown substantial effectiveness against G + ve and G- Negative bacteria, as well as certain fungi [29, 30]. Nanomaterials can be produced via biological [31, 32, 33, 34], physical [35, 36], or chemical processes [37, 38, 39]. However, very few studies focus on chemically synthesized MnO_2 nanostructures [40, 41]. Conversely, iron oxide exists in several forms, with hematite (α-Fe_2O_3), magnetite (Fe_3O_4), and maghemite (γ-Fe_2O_3) being the most stable [42,43]. Hematite, the most stable form under ambient conditions, has been used as an antibacterial agent [44]. In brief, the combination of bare γ-MnO_2 nanostars and γ-MnO_2 nanostars coated with Fe_2O_3 nanoparticles is investigated to explore the capacity to hinder bacterial growth of the nanoparticles.

2. EXPERIMENTAL

2.1 Synthesis of γ-MnO_2 nanostars

Synthesis of γ-MnO_2 nanostars and γ-MnO_2 nanostars coated with Fe_2O_3 nanoparticles: All substances used in this investigation are purchased from Sigma-Aldrich India, including sodium chlorate, manganese sulfate monohydrate, and ferric nitrate nonahydrate, and are utilized without further purification. Nano star-shaped γ-MnO_2 is synthesized as depicted in Figure 1 by dissolving sodium chlorate ($NaClO_3$) and manganese sulfate monohydrate ($MnSO_4 \cdot H_2O$) in a mole ratio of 2:1 in distilled water, as has reported in a previous paper [45]. The solutions are magnetically stirred to obtain a clear solution, then hydrothermally heated at 160 degrees Celsius for 12 hours. After filtering and washing repeatedly with distilled water, the dark brown γ-MnO_2 precipitate is desiccated at 70ºC for 6 hours. For the synthesis of γ-MnO_2 nanostars coated with Fe_2O_3 nanoparticles, ferric nitrate ($Fe(NO_3)_3 \cdot 9H_2O$) is dissolved in water and then mixed with γ-MnO_2 nanostars powder at (1:1) weight ratio; this solution is then heated for 6 hours at 150ºC. After that, the solid product is collected and cleaned repeatedly using distilled water before being heated at 400ºC for 2 hours.

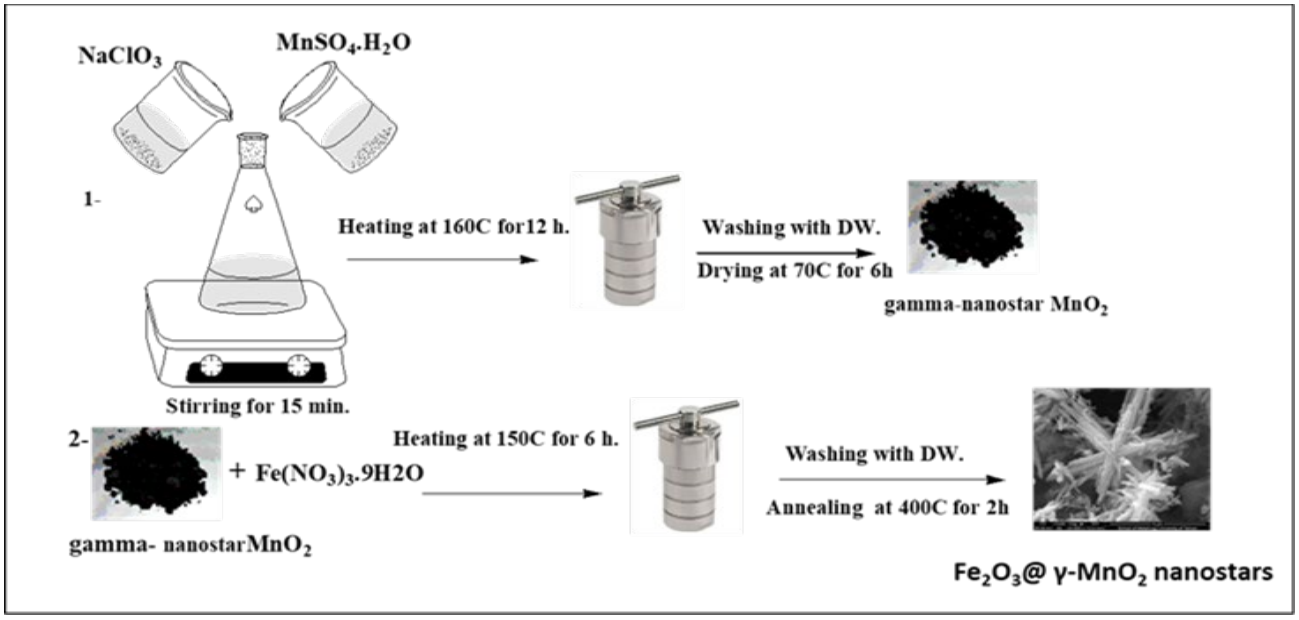

Figure 1 Graphic diagram of γ-MnO_2 nanostars coated with Fe_2O_3 nanoparticles.

2.2 Characterization

The materials are characterized using Cu Kα radiation and Japan's XRD SHIMADZU (XRD 6000) (λ=1.54180Å). The samples' morphology is examined using FE-SEM (Hitachi /S-4160 /Japan), and EDX analysis is made using (Bruker X Flash 6l10). The radical scavenging performance is studied using a UV-vis spectrophotometer.

2.3 Antibacterial Activity

The capacity to hinder bacterial growth of (γ-MnO_2 nanostars and Fe_2O_3 @γ-MnO_2) is investigated against Gram^{-ve} (*Escherichia coli* and *Salmonella*) and Gram^{+ve} (*Staphylococcus aureus* and *Bacillus subtilis*) bacterial strains using the diffusion assay in agar wells [46] using Muller-Hinton (MH) agar. Various concentrations of Fe_2O_3@γ-MnO_2 nanostars and γ-MnO_2 nanostars are separately introduced into the bored wells. The data are statistically analyzed using GraphPad Prism. The data represent the mean ± SD of three studies, with a statistically significant difference at $p<0.05$ [47].

2.4 Antioxidant Activity

The Antioxidant activity of γ-MnO_2 nanostars and Fe_2O_3 @γ-MnO_2 nanostructures is measured using the scavenging of DPPH radical method. The concentrations of the nanomaterials are 400, 600, 800, 1000 µg\ml, and ascorbic acid served as a reference.

3. RESULTS AND DISCUSSION

3.1 Generated Fe_2O_3 @γ-MnO_2 nanostructures and γ-MnO_2 nanostars

The generated Fe_2O_3 @γ-MnO_2 nanostructures and γ-MnO_2 nanostars' XRD peaks are displayed in Figures 2A and B, respectively. The pure phase of orthorhombic γ-MnO_2 is represented by all of the diffraction peaks in Figure 2A, and these peaks are consistent with the standard published data (JCPDS card No.14-0644, with lattice parameters a=6.36Aº, b=10.15Aº Aº, and c=4.09Aº) [48]. The peaks located at the crystal planes (120), (031), (131), (230), (300), (160), (421) and (003) are represented by

the values of 2θ = 22.36º, 34.36º, 37.22º, 38.78º, 42.56º, 56.14º, 65.48º and 68.82º, respectively, and no additional peaks for any more materials showing pure γ-MnO_2. In Figure 2 B, peaks located at (33.15 (104), 35.61 (110), 49.47 (024), 54.08 (116), 62.44 (214), 63.98 (300)) are indications of Fe_2O_3 Hematite, which conforms well to the standard patterns (JCPDS card No.00-033-0664) [49].

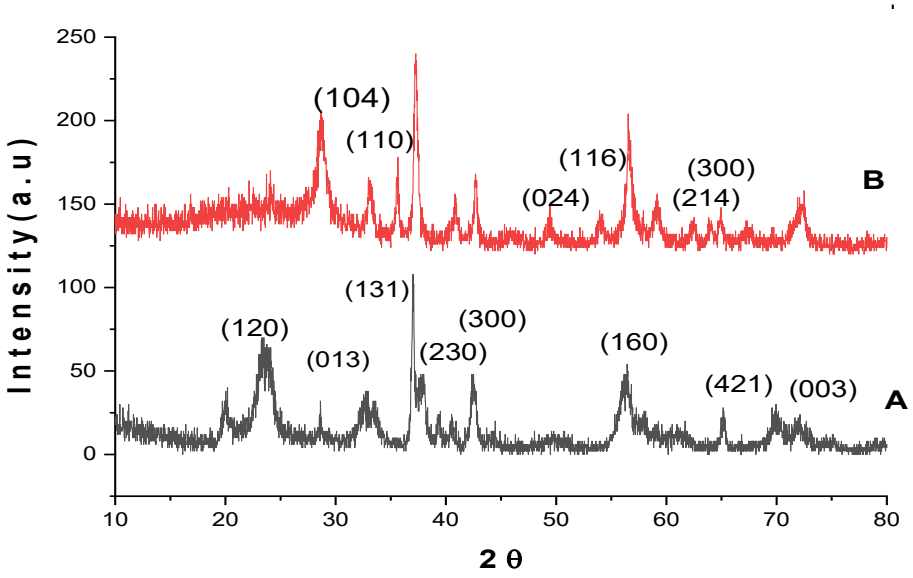

Figure 2 The X-Ray Diffraction image of (A) nanostars γ-MnO_2 and (B) nanostars γ-MnO_2 coated with Fe_2O_3 nanoparticles.

The Debye-Scherrer equation is used to calculate the crystalline size of the nanomaterials as following:

$$D = \frac{K\lambda}{\beta \cos\theta} \quad (1)$$

where D is the average crystalline size of the nanoparticles, K is the Scherrer constant related to the crystallite shape, λ is the x-ray wavelength 1.54 Å for Cu-kα and β is the full width at half maximum (FWHM). The average crystalline size calculated from Debye-Scherrer equation are 22 nm and 24 nm for γ-MnO_2 nano stars and γ-MnO_2 coated with Fe_2O_3 nanoparticles respectively.

Figure 3 demonstrates SEM descriptions of the star shapes of γ-MnO_2 nanostructure in three different magnifications. The diameters of the six-branched star-shaped γ-MnO_2 are about 140 nm close to the star's center, 55–70 nm close to its tips, and 1.5–4 μm in length. Figure 4 shows the nano γ-MnO_2 star shapes coated with tiny spherical Fe_2O_3 nanoparticles with diameters of 35-47 nm. Figure 5 shows the EDX analysis of the γ-MnO_2 nanostars coated with Fe_2O_3 nanoparticles. It clearly shows the elemental composition that includes Mn, O, and Fe. The differences in size between Scherrer's equation and the SEM is related to the fact that Scherrer measures the internal crystalline size while the measurement from SEM shows external size for agglomerated particles so it is always larger than the size from Scherrer's equation.

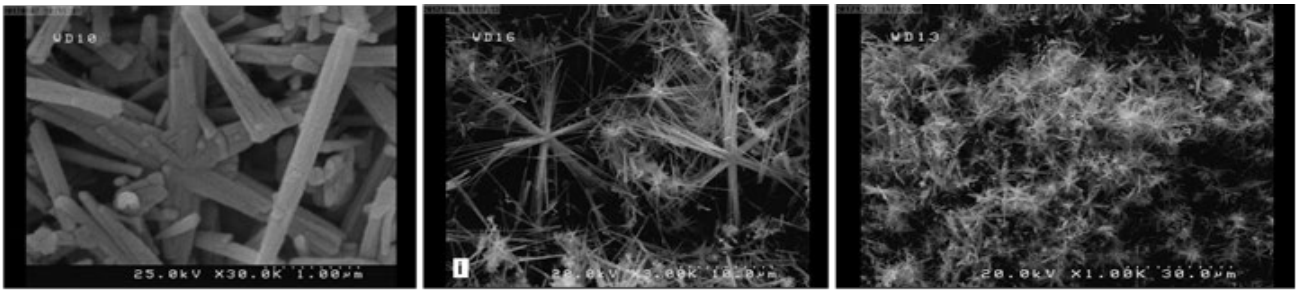

Figure 3 FE-SEM images of γ-MnO_2 nanostars.

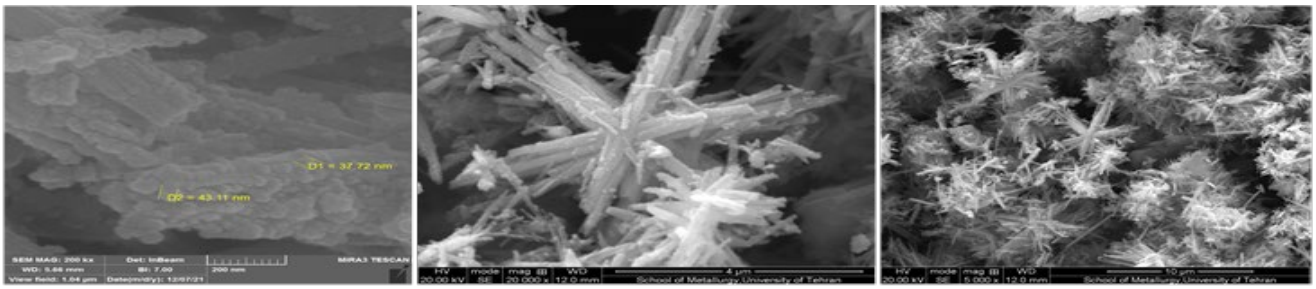

Figure 4 FE-SEM images of γ-MnO_2 nanostars coated with Fe_2O_3 nanoparticles.

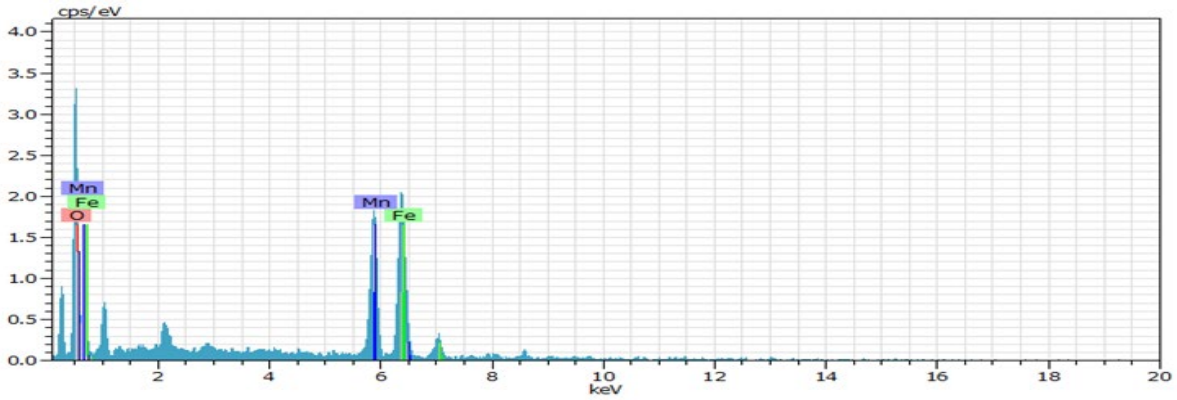

Figure 5 EDX analysis of γ-MnO_2 nanostars coated with Fe_2O_3 nanoparticles.

3.2 Antibacterial activity

The antibacterial activities of the bare γ-MnO_2 nanostars are presented in Figures 6 and 7 against *E. coli* and Salmonella, respectively, in different concentrations, and for γ-MnO_2 nanostars coated with Fe_2O_3 nanoparticles are presented in Figures 8 and 9 against *E. coli* and *Salmonella*. Respectively. The antibacterial activities for bare γ-MnO_2 nanostars and the γ-MnO_2 nanostars coated with Fe_2O_3 nanoparticles against *Bacillus subtilis* are depicted in Figure 10, and against *Staphylococcus aureus* are depicted in Figure 11. According to the values of the inhibition zones displayed in Table 1, it is evident from these figures that the γ-MnO_2 nanostars coated and uncoated with Fe_2O_3 nanoparticles have a substantial potential to combat *Salmonella and E. coli*. These samples show increased inhibition zones with increasing concentration. At the lower concentration used 400 µg /ml, the inhibition zones show some difference between the coated and uncoated samples against *E. coli*, however it is almost identical inhibition for the samples used against *Salmonella* at this same concentration. Where the inhibition zone for γ-MnO_2 nanostars against *E. coli* is 17 mm, and it is 13mm for γ-MnO_2 nanostars coated with Fe_2O_3 nanoparticles at concentration of 400 µg/ml, but the inhibition zone for γ-MnO_2 nanostars against

Salmonella is 18 mm, and it is 17 mm for γ-MnO_2 nanostars coated with Fe_2O_3 nanoparticles at concentration 400 μg/ml. However, the results are nearly identical when higher concentrations are used. The inhibition zone for γ-MnO_2 nanostars against *E. coli* is 24 mm, and it is 23 mm for γ-MnO_2 nanostars coated with Fe_2O_3 nanoparticles at a concentration of 1000 μg/ml. Whereas the inhibition zone for γ-MnO_2 nanostars against *Salmonella* is 26 mm, and it is 27 mm for γ-MnO_2 nanostars coated with Fe_2O_3 nanoparticles at a concentration of 1000 μg/ml. However, these nanostructures do not exhibit any antibacterial action against *S. aureus* and *B. subtilis*; this phenomenon can be explained by the bacterial cell wall structures of Gram-positive and Gram-negative bacterial species. The bacterial species classified as Gram-negative have an outer membrane that includes lipopolysaccharides and a peptidoglycan layer [52,53]. In contrast, the bacterial species categorized as Gram-positive have an outer membrane that consists of peptidoglycans, lipoteichoic acid, and teichoic acid [54,55]. The proposed antibacterial mode of action of nanomaterials is believed to arise from the generation of reactive oxygen species (ROS), such as hydrogen peroxide (H_2O_2), hydroxyl free radicals (·OH), or superoxide anion radicals ($\cdot O^{2-}$) [56]. The extensive surface area can increase the production of ROS; these molecules can damage biomolecules by their pronounced oxidation potential [57-60].

The antibacterial inhibition of MnO_2 nanoparticles is explained by some mechanisms; the first mechanism is that when MnO_2 nanoparticles are attached to the bacterial membrane it will release (Mn^{+2}) and oxygen. The manganese ions can interact with some functional groups in the proteins of the bacterial membrane, which will cause inactivation of enzymes, and then the membrane will be disrupted. The other mechanism is the generation of reactive oxygen species (ROS). These actions will disrupt the cell membrane of the bacteria, leading to leakage of cell contents [61]. the smallest the nanomaterials, the better the penetration of the cell membrane. We can see that the uncoated MnO_2 shows better antibacterial inhibition than the coated samples, maybe due to the larger overall size of the coated samples, or maybe due to coating the MnO_2 surface with another material, which will hinder the release of (Mn^{+2}) and oxygen.

Table 1 Inhibition zone values for the γ-MnO_2 nanostars shape and Fe_2O_3@γ-MnO_2.

Sample	A	B	C	D	E
Fe_2O_3@γ-MnO_2 against *E. coli*	6	13	18	19	23
Fe_2O_3@γ-MnO_2 against *Salmonella*	6	17	20	21	26
γ-MnO_2 nanostars against *E. coli*	6	17	18	19	24
γ-MnO_2 nanostars against *Salmonella*	6	18	19	20	27

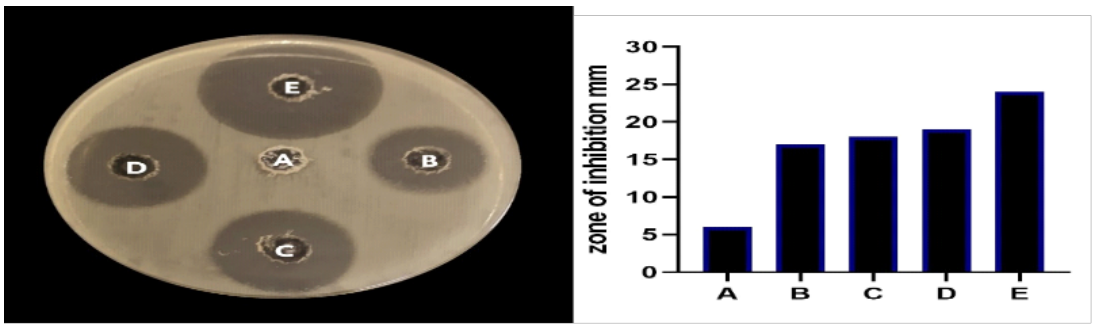

Figure 6 Antibacterial activity of γ-MnO_2 nanostars against *Escherichia coli*. In different concentrations, (A) control (solvent only), (B) 400(µg /ml), (C) 600(µg/ml), (D) 800(µg /ml), and (E) 1000 (µg/ml).

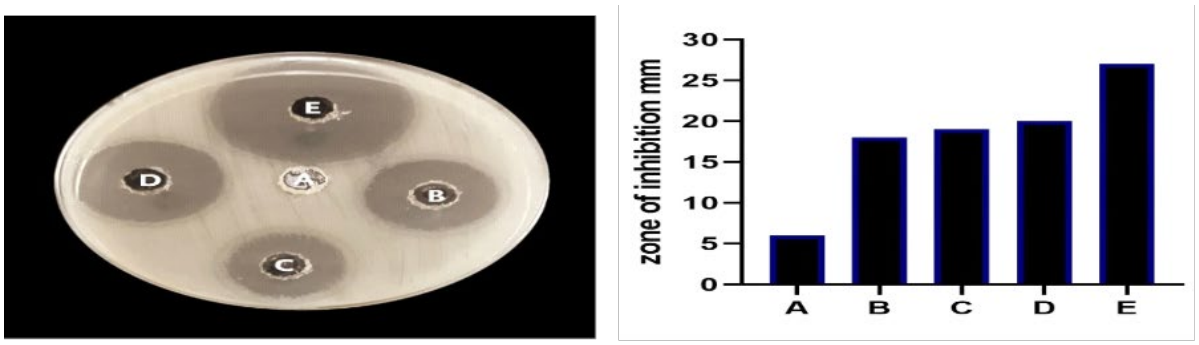

Figure 7 Antibacterial activity of γ-MnO_2 nanostars against *Salmonella* in different concentrations (µg /ml), (A) control (solvent only), (B) 400, (C) 600, (D) 800, and (E) 1000.

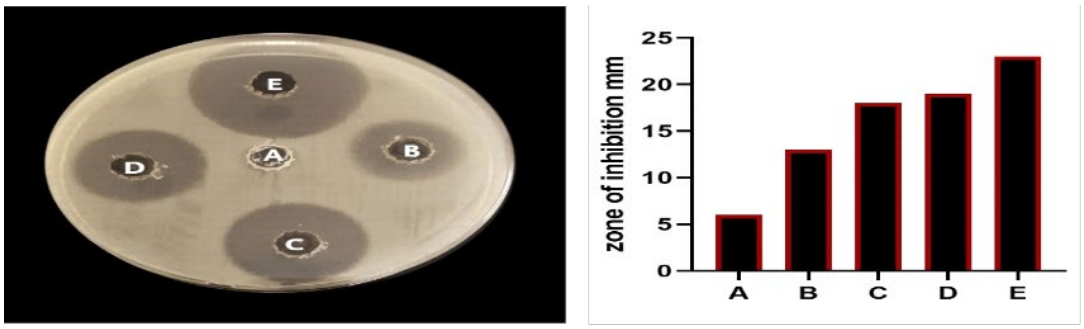

Figure 8 Antibacterial activity of Fe_2O_3 @γ-MnO_2 against *Escherichia coli* in different concentrations (µg /ml), (A) control (solvent only), (B) 400, (C) 600, (D) 800, and (E) 1000.

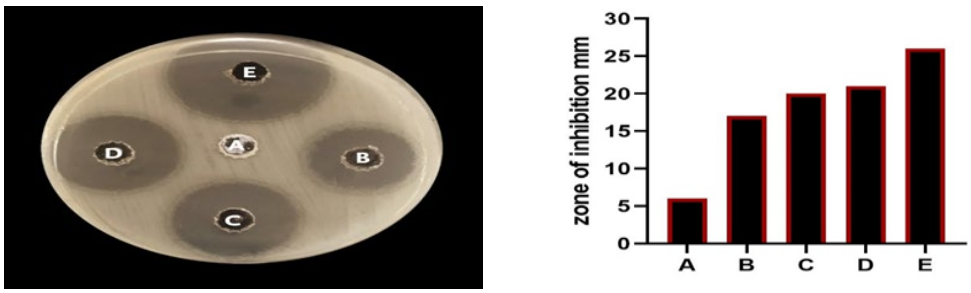

Figure 9 Antibacterial activity of Fe_2O_3 @γ-MnO_2 against *Salmonella* in different concentrations (µg/ml), (A) control (solvent only), (B) 400, (C) 600, (D) 800, and (E) 1000.

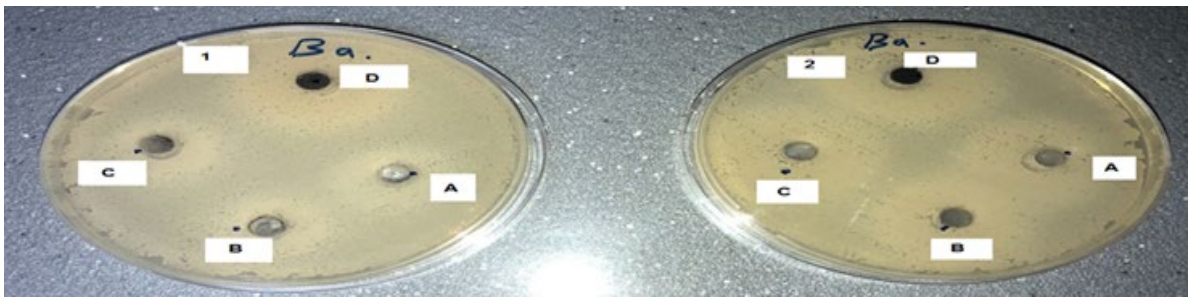

Figure 10 Antibacterial activity of (1) Fe_2O_3 @γ-MnO_2 and (2) γ-MnO_2 nanostars shape against *Bacillus subtilis* in different concentrations, (µg /ml) (A) 400, (B) 600, (C) 800, and (D) 1000.

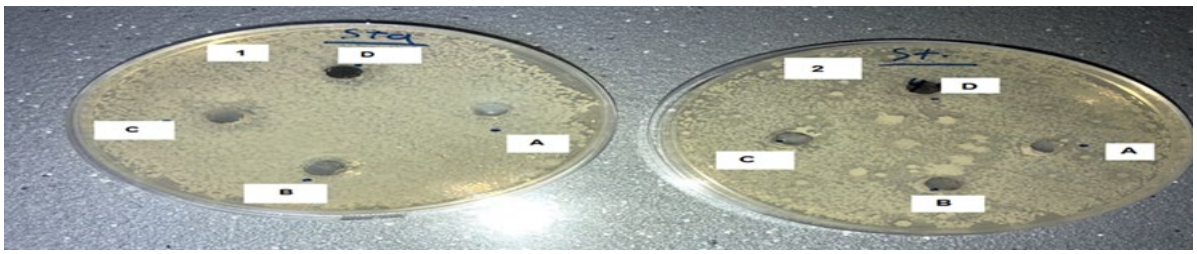

Figure 11 Antibacterial activity of (1) Fe_2O_3 @γ-MnO_2 and (2) γ-MnO_2 nanostars against *Staphylococcus aureus*. In different concentrations (µg /ml): (A) 400, (B) 600, (C) 800, and (D) 1000.

3.3 Antioxidant Activity

The DPPH scavenging activity (% inhibition) is investigated using varying concentrations (200, 400, 500, 500,800, and 1000 µg / ml) of both γ-MnO_2 nanostars and Fe_2O_3 @ γ-MnO_2 nanostructure. The absorbance at 517 nm is measured using ascorbic acid as a reference [51].

The ability of the DPPH radical scavenging system is derived using the following formula:

$$\%DPPH\ scavenging\ activity\ (\%\ Inhibition) = \frac{A_{control} - A_{test}}{A_{control}}\ x\ 100 \quad (1)$$

In this case, a test means sample absorbance, and A control corresponds to control absorbance. The antioxidant activities of the synthesized nanomaterials are expressed as the IC_{50}, where the IC_{50} value is the concentration of the antioxidant required to reduce the DPPH free radical by 50%. The lower the value of IC_{50}, the more enhanced the inhibition action of the antioxidant. The scavenging percent of the samples at various concentrations is depicted in Figure 12. The findings reveal the IC_{50} values of γ-MnO_2 nanostars, Fe_2O_3 @ γ-MnO2 nanostars, and ascorbic acid, which are 962, 766, and 424 µg\ml, respectively. These outcomes reveal that the Fe_2O_3 @γ-MnO_2 nanostars have enhanced radical scavenging performance compared to bare γ-MnO2 nanostars. This could be because this material can donate more electrons and inhibit the DPPH free radical [31]. The Fe_2O_3@γ-MnO_2 nanostars and bare γ-MnO_2 nanostars show % inhibition (68.6% and 52%), respectively at the highest concentration (1000 µg/ml), while ascorbic acid shows % inhibition (93%) at the same concentration.

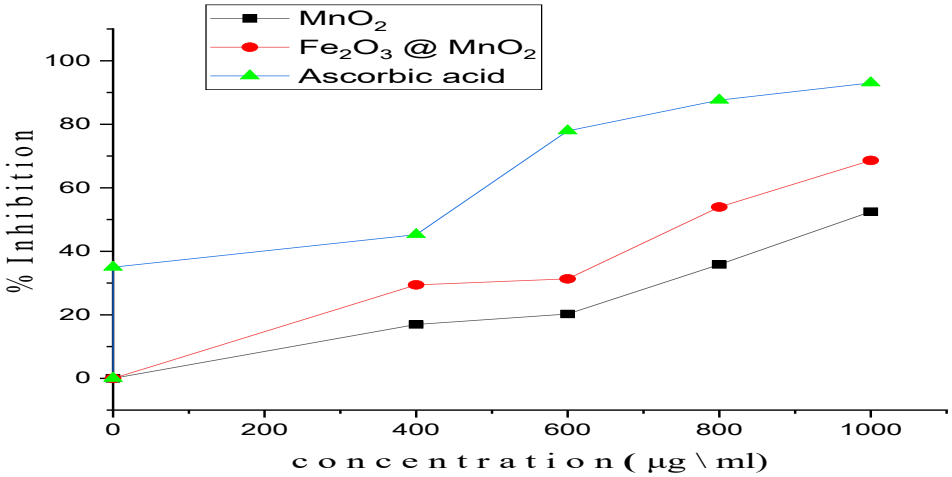

Figure 12 Antioxidant activity of γ-MnO_2 nanostars, Fe_2O_3 @ γ-MnO_2 nanostars, and ascorbic acid on DPPH radical.

4. CONCLUSIONS

Synthesis of γ-MnO_2 nanostars and γ-MnO_2 nanostars coated with Fe_2O_3 nanoparticles is successfully achieved using the hydrothermal synthesis route. With the highest inhibitory zone, the materials exhibit notable antibacterial action against bacterial species classified as Gram-negative (27mm), but don't show antibacterial action against the bacterial species categorized as Gram-positive; the capacity to hinder bacterial growth of the materials is almost the same. This result is significant since G^{-ve} bacteria are more resistant to antibiotics than G^{+ve}. The γ-MnO_2 nanostars coated with Fe_2O_3 nanoparticles exhibite enhanced radical scavenging performance compared to bare γ-MnO_2 nanostars.

Funding
The study is self-funded.

Conflict of Interest
There is no conflict of interest.

Acknowledgments
The authors would appreciate the insight of all reviewers and would appreciate their feedback, which help to improve the quality and clarity of the paper.

Ethical Considerations
All ethical guidelines are strictly followed throughout the study. The authors affirm that no data fabrication, falsification, plagiarism, or research misconduct have occurred. Ethical approval is granted by the research Ethics committee / University of Baghdad/ College of Agricultural Engineering Sciences (Approval No. 111, dated June 30, 2025).

References

[1] R. Ali, R., Shanan, Z. J., Saleh, G. M., and Abass, Q. Iraqi Journal of Science, 50(2020) 266-276.
[2] I. Abbas AL-Essawi, and H. M. Mahmood, J. of Nanostruct. 14 (2024) 1029 https://doi.org/10.22052/JNS.2024.04.004
[3] S. Sathiyaraj, G. Suriyakala, A. D. Gandhi, R. Babujanarthanam, K. S.Almaary, T. W. Chen, and Kaviyarasu, J. of Inf. and Pub. Heal., 14 (2021) 1842 https://doi.org/10.1016/j.jiph.2021.10.007

[4] G. A. Nasir, I. A. Khudhair, M. A. Najm, and H. M. Mahmood, Al-Raf. J.of Medi. Sci., 3 (2022) 71 https://doi.org/10.54133/ajms.v3i.88
[5] G. E. Yılmaz, I. Göktürk, M. Ovezova, F. Yılmaz, S.Kılıç, and A. Denizli, Hyg., 3 (2023) 269 https://doi.org/10.3390/hygiene3030020
[6] N. Sher, D.H.M. Alkhalifah, M. Ahmed, N. Mushtaq, F. Shah, F. Fozia, R.A.Khan, W.N. Hozzein and M.A.M. Aboul-Soud, Mole. 27 (2022) 7895 https://doi.org/10.3390/molecules27227895
[7] G. Nasir, M. Najm, H. Mahmood. J Nanostruct 15 (2025) 249 DOI: 10.22052/JNS.2025.01.024
[8] S. S. Salman, A. T. Al-Douri, A. A. Hadi, S. J., M. Alnajm. EXP. THEO. NANOTECHNOLOGY 9 (2025) 361 https://doi.org/10.56053/9.2.361
[9] C. R. Mendes, G. Dilarri, C. F. Forsan, V. D. Sapata, M. R., Lopes, P. R. M., de, P. B. Moraes and E. D. Bidoia ,Scientific Reports 12 (2022) 2658 https://doi.org/10.1038/s41598-022-06657-y
[10] A. B. Younis, V. Milosavljevic, T. Fialova, K. Smerkova, H. Michalkova, P.Svec, and K. Dolezelikova, BMC Microbiol 23 (2023) 207 https://doi.org/10.1186/s12866-023-02955-1
[11] K. S. Khashan, G. M. Sulaiman, F. A. Abdulameer, S. Albukhaty, M. A. Ibrahem, T. Al-Muhimeed, and A. A. Al Obaid, Appl. Sci. 11 (2021) 4623 https://doi.org/10.3390/app11104623
[12] G. L. A. Raheem, G.A. Nasir, M. M. M. Alshammari, and A. Ghasemian, . Malay. J. Biochem. Mol. Biol. 23 (2020) 15 https://www.mjbmb.org/general-3
[13] S. Khamsanga, Pornprasertsuk, R., Yonezawa, T., Mohamad, A. A., & Kheawhom, S. Sci Rep ,9 (2019) 8441 https://doi.org/10.1038/s41598-019-44915-8
[14] A.Umar, A. A., Ibrahim, R. Kumar, H.B, Albargi, W. Zeng, M. A.M. Alhmami, M. A. Alsaiari, S. Baskoutas, Materials Letters 286 (2021) 129232 DOI:10.1016/j.matlet.2020.129232
[15] A. Umar, A. A.Ibrahim , R. Kumar, H. Algadi, H. Albargi, F. Ahmad, W. Zeng, and M.S. Akhtar 11 (2021) 860 https://doi.org/10.3390/coatings11070860
[16] S. Datta, A. Dey, N. R. Singha, and S. Roy, Mater Ren. Sust. Energy 9 (25) (2020) 1 https://doi.org/10.1007/s40243-020-00185-3
[17] S. Panimalar, S. Logambal, R. Thambidurai, C. Inmozhi, R. Uthrakumar, A. Muthukumaran, R. A. Rasheed, M. K. Gatashes, A. Raja, J. Kennedy and K. Kaviyarasu, Envi. Res. 205 (2022) 112560 https://doi.org/10.1016/j.envres.2024.120673
[18] S. M. Husnain, U. Asim, A. Yaqub, F. Shahzad, and N. Abbas, New J. of Chem. 44 (2020) 6096 https://doi.org/10.1039/C9NJ06392G
[19] A. Greene, J. Hashemi, and Y. Kang, Nanotech. 32 (2020) 025713 DOI:10.1088/1361-6528/abb626
[20] H. Y. Xia, B. Y. Li, Y. Zhao, Y. H. Han, S. B. Wang, A. Z. Chen, and R.K. Kankala, Co. Chem. Rev. 464 (2022) 214540 https://doi.org/10.1016/j.ccr.2022.214540
[21] S.D. Raut, H.R. Mane, N.M. Shinde, D. Lee, S.F. Shaikh, K.H. Kim, H.J. Kim, A.M. Al-Enizi and R.S. Mane, New J. of Chem. 41 (2020) 17864 doi 10.1039/d0nj03792c
[22] Y. Kumar, S. Chopra, A. Gupta, Y. Kumar, S.J. Uke, and S.P. Mardikar, Mat. Sci. for Energy Tech. 3 (2020) 566 https://doi.org/10.1016/j.mset.2020.06.002
[23] F. Wang, Y. Zheng, Q. Chen, Z. Yan, D. Lan, E. Lester, and T. Wu, : A review, Co. Chem. Rev. 500 (2024) 215537 https://doi.org/10.1016/j.ccr.2023.215537
[24] P.M. De Wolff, Acta Cryst. 12 (1959) 341 https://doi.org/10.1107/S0365110X59001001
[25] H. Lu, X. Zhang, S.A. Khan, W. Li, and L. Wan, Fron.in Micro. 12 (2021) 761084 https://doi.org/10.3389/fmicb.2021.761084
[26] A. M. Díez-Pascual, Nanomaterials 10 (2020) 2315 https://doi.org/10.3390/nano10112315
[27] S. O. Ogunyemi, M. Zhang, Y. Abdallah, T. Ahmed, W. Md. A. Ali, C. Yan, Y. Yang, J.Chen and B. Li, , Front Microbiol 11 (2020) 588326 Doi:10.3389/fmicb.. 2020.588326
[281]T. Al-Mohammed, and H. Mahmood (2024). Carbapenem resistance related to biofilm formation and pilin genes in clinical Pseudomonas aeruginosa Isolates, Iraqi Journal of Pharmaceutical Sciences 33 (2024) 72 doi.org/10.31351/vol33iss1pp72-78
[29] K. Kala, M. S., Jeyalakshmi, S.Mohandoss, and R. Surfaces and Interfaces 40 (2023) 103136 https://doi.org/10.1016/j.surfin.2023.103136

[30] A. A. Shareef, Z. A. Hassan, M. A. Kadhim, and A. A. Al-Mussawi, Bag. Sci. J. 19 (2022) 55 https://doi.org/10.21123/bsj.2022.19.3.0460
[31] M. F. Altaee, L. A. Yaaqoob, and Z. K. Kamona, Iraqi J. of Sci. 61 (2020) 2888 https://doi.org/10.24996/ijs.2020.61.11.12
[32] A. A. R. Niema, E. M. Abbas, and N. K. Abdalameer, Digest Journal of Nanom. & Biostru. (DJNB) 16 (2021) 1479 DOI:10.15251/djnb.2021.164.1479
[33] H. H. Bahjat, R. A. Ismail, G. M. Sulaiman, and M. S. Jabir, J. of Inorg. and Organ. Poly. and Mats. 31 (2021) 36649 DOI:10.1007/s10904-021-01973-8
[34] A. J. Katafa, and M. K. Hamid, Iraqi J. of Sci. 61 (2020) 540 https://doi.org/10.24996/ijs.2020.61.3.10
[35] M. K. Mohammed, M. R. Mohammad, M. S. Jabir, and D. S. Ahmed, In IOP Conference Series: Mat. Sci. and Eng. 757 (2020) 012028 DOI:10.1088/1757-899X/757/1/012028.
[36] M.S. Jabir, T. M. Rashid, U. M. Nayef, S. Albukhaty, F. A. AlMalki, J.Albaqami, A. A. AlYamani, Z. J. Taqi, and G. M. Sulaiman, Bioinor. Chem. and Appli. 1 (2022) 2663812 https://doi.org/10.1155/2022/2663812.
[37] T. Du, S. Chen, J. Zhang, T. Li, P. Li, J. Liu, X. Du and S. Wang, Nanomat. 10 (2020) 1545 Doi10.3390/nano10081545
[38] M. F. Warsi, K. Chaudhary, S. Zulfiqar, A.Rahman, I. A. Al Safari, H.M. Zeeshan, P.O. Agboola, M. Shahid and M. Suleman, Cera. Interl. 48 (2022) 4930 https://doi.org/10.1016/j.ceramint.2021.11.031
[39] Y. Yan, N. Jiang, X. Liu, J. Pan, M. Li, C. Wang, P.H.C. Camargo and J. Wang, Front. in Bioeng. and Biotechnol. 9 (2021) 57 https://doi.org/10.3389/fbioe.2021.788574
[40] A. Sajjad, S. Hussain, G.H. Jaffari, S. Hanif, M.N. Qureshi, and M. Zia, Nano Trends 2 (2023) 100010 https://doi.org/10.1016/j.nwnano.2023.100010
[41] Haneen Khaled Naji Al-Samarrai, Osama Nadhom Nijris, Mohammed Fadhil AboKsou, EXP. THEO. NANOTECHNOLOGY 9 (2025) 529 https://doi.org/10.56053/9.4.529
[42] S. Faisal, S. Sadiq, M.Mustafa, M. H. Khan, M. Sadiq, Z. Iqbal, and M. Khan, RSC Sust. 1 (2023) 139 DOI https://doi.org/10.1039/D2SU00044J
[43] Z. H. Raheem, and A. M. A. Al Sammarraie, , AIP Conf. Proc. 2213 (2020) 020187 https://doi.org/10.1063/5.0000246
[44] Saeed S. Ba Hashwan, Mohd Haris Md Khir, Illani Mohd Nawi, Muzamil A. Hassan, Abdullah S. Algamili, Hussein Shutari, EXP. THEO. NANOTECHNOLOGY 9 (2025) 539 https://doi.org/10.56053/9.4.539
[45] T.J. Hossain, European J.l of Micr. and Imm. 14 (2024) 97 doi: 10.1556/1886.2024.00035
[46] M. Sindhuja, S. Padmapriya, V. Sudha, and S. Harinipriya, Inter. J.of Hyd. En. 44 (2019) 5389 https://doi.org/10.1016/j.ijhydene.2018.08.123
[47] S. Vihodceva, A. Šutka, M. Sihtmäe, M. Rosenberg, M. Otsus, I. Kurvet, L. Bikse, A.Kahru and K. Kasemets, Nano. 11 (2021) 652 https://doi.org/10.3390/nano11030652
[48] R. Ali, Z.J. Shanan, G.M. Saleh, and Q. Abass, Iraqi J. of Sci. 61 (2020) 266 https://doi.org/10.24996/ijs.2020.61.2.9
[49] Maksood Adil Mahmoud Al-Doori, Nahedh Ayad Faris, Noor Adnan Mahmood, Asaad T. Al-Douri, Luay Mannaa ibrahim, Amna M. Al-Tikrity, EXP. THEO. NANOTECHNOLOGY 9 (2025) 555 https://doi.org/10.56053/9.4.555
[50] H. M. Mahmood, M.M. Ali, B.J. Aldahham, B.J., and L.M. Al-Ani. Hyb. Advan. 11 (2025) 99 https://doi.org/10.1016/j.hybadv.2025.100567S
[51] M. A. Alden, and L. A. Yaaqoob, Iraqi j. of Agri. Sci. 53 (2022) 27 https://doi.org/10.36103/ijas.v53i1.1502
[52] M. Rahmat, H.N. Bhatti, A. Rehman, H. Chaudhry, M. Yameen, M. Iqbal, S.H. Al-Mijali, N. Alwadai, M. Fatima and M. Abbas, Arab. J. of Chem. 14 (2021) 103415 https://doi.org/10.1016/j.arabjc.2021.103415
[53] M.A. Najm, G.A.Nasir, H. M. Mahmood, Agricultural Biotechnology Journal 17 (2025) 217 https://doi.org/10.22103/jab.2025.24920.1672

[54] L. Wang, H. He, C. Zhang, L. Sun, S. Liu, and S. Wang, J. of Envi.Sci. 41 (2016) 112 DOI: 10.1016/j.jes.2015.04.026
[55] K. S. Khashan, B. A. Badr, G. M. Sulaiman, M. S. Jabir, and S.A. Hussain, J. of Phys.: Conference Series, 1795 (2020) 012040 DOI 10.1088/1742-6596/1795/1/012040
[56] H. AlKhafaji, R. H. Mohsin, and M.J. Kadhim, Bas. J. of Agri. Sci. 37 (2024) 249 DOI:10.37077/25200860.2024.37.2.19
[57] Asaad T. Al-Douri, Alaa A. Khaleel, Luay Mannaa ibrahim, Abeer Talib Abdulqader, Ammr Khalid Shihab, Mustafa Khaleel Ibrahim, Maksood Adil Mahmoud Al-Doori, EXP. THEO. NANOTECHNOLOGY 9 (2025) 563 https://doi.org/10.56053/9.4.563
[58] M.Q. Mohammed, A.H. Shugran, EXP. THEO. NANOTECHNOLOGY 10 (2026) 13 https://doi.org/10.56053/10.1.13
[59] S.A. Alnuaimi, D. Vaishnavi, H. G. Hameed. EXP. THEO. NANOTECHNOLOGY 9 (2025) 513 https://doi.org/10.56053/9.3.513.
[60] N. M. Slaber, J. S. Kith, EXP. THEO. NANOTECHNOLOGY 9 (2025) 9 https://doi.org/10.56053/9.1.9
[61] I. Fitriannisa, H.T. Draviana, , C. P.Hsieh, M.Saukani, K. Y. Tzou, , and T. R .Kuo. International journal of molecular sciences 26 (2025) 9104 https://doi.org/10.3390/ijms26189104

© 2026 The Authors. Published by LPCMA (https://etnano.com). This article is an open access article distributed under the terms and conditions of the Creative Commons Attribution license (http://creativecommons.org/licenses/by/4.0/).